

Wavefront depinning transition in discrete one-dimensional reaction-diffusion systems

A. Carpio¹ and L. L. Bonilla²¹Departamento de Matemática Aplicada, Universidad Complutense de Madrid,
28040 Madrid, Spain²Departamento de Matemáticas, Escuela Politécnica Superior, Universidad Carlos III de Madrid,
Avenida de la Universidad 30, 28911 Leganes, Spain
(April 14, 2024)

Pinning and depinning of wavefronts are ubiquitous features of spatially discrete systems describing a host of phenomena in physics, biology, etc. A large class of discrete systems is described by overdamped chains of nonlinear oscillators with nearest-neighbor coupling and controlled by constant external forces. A theory of the depinning transition for these systems, including scaling laws and asymptotics of wavefronts, is presented and confirmed by numerical calculations.

82.40.-g; 05.45.-a

Spatially discrete systems describe physical reality in many different fields: propagation of nerve impulses along myelinated fibers [1,2], pulse propagation through cardiac cells [2], calcium release waves in living cells [3], sliding of charge density waves [4], superconductor Josephson array junctions [5], motion of dislocations in crystals [6], atoms adsorbed on a periodic substrate [7], arrays of coupled diode resonators [8], and weakly coupled semiconductor superlattices [9,10]. A distinctive feature of discrete systems (not shared by continuous ones) is the phenomenon of wavefront pinning: for values of a control parameter in a certain interval, wavefronts joining two different constant states fail to propagate [2]. When the control parameter surpasses a threshold, the wavefront depins and starts moving [1,4,6,10]. The existence of such thresholds is thought to be an intrinsically discrete fact, which is lost in continuum approximations. The characterization of propagation failure and front depinning in discrete systems is thus an important problem, which is still poorly understood despite the numerous inroads made in the literature [1,3,4,6,11-13].

In this Letter, we study front depinning for infinite one-dimensional nonlinear spatially discrete reaction-diffusion (RD) systems. The nature of the depinning transition depends on the nonlinearity of the model, and is best understood as propagation failure of the traveling front. Usually, but not always, the wavefront profiles become less smooth as a parameter F (external field) decreases. They become discontinuous at a critical value F_c . Below F_c , the front is pinned at discrete positions corresponding to a stable steady state. Fig. 1 shows wavefront profiles near the critical field. Individual points undergo abrupt jumps at particular times, which gives the misleading impression that the motion of the discrete fronts proceeds by successive jumps. Wavefront velocity scales with the field as $(F - F_c)^{1/2}$. For exceptional nonlinearities, the wavefront does not lose continuity as the field decreases. In this case, there is a continuous transition between wavefronts moving to the left for $F > 0$ and moving to the right for $F < 0$: as for continuous systems, front pinning occurs only at a single field $F = 0$.

Wavefront velocity scales then linearly with the field. We discuss the characterization of the critical field (including analytical formulas in the strongly discrete limit), describe depinning anomalies (discrete systems having zero critical field), and give a precise characterization of stationary and moving fronts near depinning (including front velocity) by singular perturbation methods. Our approximations show excellent agreement with numerical calculations.

We consider chains of diffusively coupled overdamped oscillators in a potential V , subject to a constant external force F :

$$\frac{du_n}{dt} = u_{n+1} - 2u_n + u_{n-1} + F - A g(u_n); \quad (1)$$

Here $g(u) = -V'(u)$ presents a 'cubic' nonlinearity, such that $A g(u) - F$ has three zeros, $U_1 < U_2 < U_3$ in a certain force interval ($g'(U_i(F=A)) > 0$ for $i = 1, 3$, $g'(U_2(F=A)) < 0$). Provided $g(u)$ is odd with respect to $U_2(0)$, there is a symmetric interval $F_j - F_c$ where the wavefronts joining the stable zeros $U_1(F=A)$ and $U_3(F=A)$ are pinned. For $F_j > F_c$, there are smooth traveling wavefronts, $u_n(t) = u(n - ct)$, with $u(-1) = U_1$ and $u(1) = U_3$ [14,15]. The velocity $c(A; F)$ depends on A and F and it satisfies $cF < 0$ and $c \neq 0$ as $F_j \neq F_c$ [15]. Examples are the overdamped Frenkel-Kontorova (FK) model ($g = \sin u$) [16] and the quartic double well potential ($V = (u^2 - 1)^2/4$). Less symmetric nonlinearities yield a non-symmetric pinning interval and our analysis applies to them with trivial modifications.

Critical field. Stationary and traveling wavefronts cannot coexist for the same value of F [15]. This follows from a comparison principle for (1) [17]. Pinning can be proved using stationary sub and supersolutions, which can be constructed provided the stationary solution is linearly stable. The largest eigenvalue of the linearization of (1) about a stationary profile $u_n(A; F)$, $u_n(t) = u_n(A; F) + v_n e^{\lambda t}$, is given by

$$\lambda(A; F) = \max_n \frac{\sum_{p=1}^P (v_{n+1} - v_n)^2 + A g''(u_n(A; F)) v_n^2}{v_n^2}; \quad (2)$$

over a set of functions v_n which decay exponentially as $n \rightarrow \infty$. The critical eld is uniquely characterized by $(A; F_c) = 0$ and $(A; F) < 0$ for $F < F_c$. Thus two facts distinguish the depinning transition: (i) one eigenvalue becomes zero, and (ii) stationary and moving wavefronts cannot coexist for the same values of the eld.

Equation (2) shows that the critical eld is positive for large A and typical nonlinearities. In fact, consider the FK potential. For $F = 0$ there are two stationary solutions which are symmetric with respect to U_2 , one taking on the value U_2 (unstable dislocation), and the other one having $u_n \neq U_2$ (stable dislocation) [18]. For large A , the stable dislocation has $g^0(u_n) > 0$ for all n , and (2) gives $(A; 0) < 0$. Since $(A; F_c) = 0$, this implies that the critical eld is nonzero. (A different proof can be obtained using the comparison principle [1,10]). As $A > 0$ decreases, several u_n may enter the region of negative slope $g^0(u)$: the number of points with $g^0(u_n) < 0$ increases as A decreases. It is then possible to have $(A; 0) = 0$, i.e. $F_c = 0$, for a discrete system! Examples of this pinning anomaly will be given below.

If $F > 0$, the stable dislocation is no longer symmetric with respect to U_2 . If F is not too large, all $u_n(A; F)$ avoid the region of negative slope $g^0(u) < 0$. For large A and F and the generic potentials above mentioned, we have observed numerically that $g^0 < 0$ for a single point, labelled $u_0(A; F)$. This property persists until F_c is reached. How does F_c depend on A ? For $g = \sin u$, it is well known that F_c vanishes exponentially fast as A goes to zero (the continuum limit). This was conjectured by Indenbom [19] on the basis of a continuum approximation, and numerically checked by Hobart [18] in the context of the Peierls stress and energy for dislocations. More recently, Kladko et al [11] derived the formula $F_c = C \exp(-\frac{2}{A})$ by means of a variational argument. This argument can be used for other potentials and it suggests that $F_c = C e^{-\frac{2}{A}}$ as $A \rightarrow 0+$ (with positive C and independent of A) holds for a large class of nonlinearities [11]. King and Chapman have obtained an analogous result [13] using exponential asymptotics for the FK potential, $F_c = C e^{-\frac{2}{A}}$ and the wavefront velocity after depinning, $c = \frac{2}{(F^2 - F_c^2)^{1/2}} A$. This later result agrees with the scaling law $c = F^{-1/2}$, found in a large class of discrete RD equations [11,12].

Anomalies of pinning. Despite widespread belief, it is not true that $F_c > 0$ for all discrete systems. Using the characterization $(A; F_c) = 0$, it is possible to see that having a zero critical eld is equivalent to having a one-parameter family of continuous increasing stationary profiles $u_n = u(n)$ satisfying $u(x+1) + u(x-1) - 2u(x) = A g(u(x))$, with $u(-1) = U_1, u(1) = U_3$. In this case, a standard perturbation argument yields a wavefront speed having the same scaling as the continuum approximation to the discrete system, $c = C F$ as $F \rightarrow 0$. An example of nonlinearity presenting this anomalous pinning [20] can be obtained from $u(x) = \tanh x$: it obeys the above equation with $A = 1, U_1 = -1, U_3 = 1$ and

$g(u) = 2 \tanh^2(1) u (1 - u^2) = [1 - \tanh^2(1) u^2]$. Furthermore the wavefront velocity after depinning obeys the relation, $c = 3F = 2$ as $F \rightarrow 0$. Thus nonlinearities presenting anomalous depinning belong to a different universality class: the wavefront velocity has a critical exponent 1 (and $F_c = 0$) instead of 1/2, which is the usual case for discrete RD systems (having $F_c > 0$).

Asymptotic theory of wavefront depinning. We shall study the depinning transition in the strongly discrete limit $A \rightarrow \infty$, in which the structure of the wavefront is particularly simple. Firstly, consider the symmetric stationary profile with $u_n \neq U_2$ for $F = 0$. The front profile consists of two tails with points very close to U_1 and U_3 , plus two symmetric points u_0, u_1 in the gap region between U_1 and U_3 . As $F > 0$ increases, this profile changes slightly: the two tails are still very close to U_1 ($F \rightarrow 0$) and U_3 ($F \rightarrow 0$). As for the two middle points, u_1 gets closer and closer to U_3 whereas u_0 moves away from U_1 . This structure is preserved by the traveling fronts above the critical eld: there is only one active point most of the time, which we can adopt as our u_0 . Then we can approximate $u_1 \rightarrow U_1, u_1 \rightarrow U_3$ in (1), thereby obtaining

$$\frac{du_0}{dt} = U_1 \frac{F}{A} + U_3 \frac{F}{A} - 2u_0 - A g(u_0) + F: \quad (3)$$

This equation has three stationary solutions for $F < F_c$, two stable and one unstable, and only one stable stationary solution for $F > F_c$. The critical eld F_c is such that the expansion of the right hand side of (3) about the two coalescing stationary solutions has zero linear term, $2 + A g^0(u_0) = 0$, and

$$2u_0 + A g(u_0) = U_1 \frac{F_c}{A} + U_3 \frac{F_c}{A} + F_c: \quad (4)$$

These equations for F_c and $u_0(A; F_c)$ have been solved for the FK potential, for which $u_0 = \cos^{-1}(2/A)$ and $U_1 + U_3 = 2 \sin^{-1}(F_c/A) + 2$. The results are depicted in Fig. 2, and show excellent agreement with the numerical solution of (1) for $A > 10$. Our approximation performs less well for smaller A , and it breaks down at $A = 2$ with the prediction $F_c = 0$. Notice that $F_c(A) \sim A$ as A increases. In practice, only steady solutions are observed for very large A .

Let us now construct the profile of the traveling wavefronts after depinning, for F slightly above F_c . Then $u_0(t) = u_0(A; F_c) + v_0(t)$ obeys the following equation:

$$\frac{dv_0}{dt} = (F - F_c) + A g^0(u_0) \frac{v_0^2}{2}; \quad (5)$$

where we have used $2 + A g^0(u_0) = 0$, (4) and ignored terms of order $(F - F_c)^2$ and higher. This equation has the (outer) solution

$$v_0(t) = \frac{s}{2(F - F_c)} \tan \frac{r}{2} \frac{A g^0(u_0) j (F - F_c)}{2} (t - t_0); \quad (6)$$

which is very small most of the time, but it blows up when the argument of the tangent function approaches $\pi/2$. Thus the outer approximation holds over a time interval $(t - t_0) \leq \frac{1}{2} \sqrt{\frac{A}{2}} \frac{1}{(F - F_c)^{1/2}}$, which equals $\frac{1}{2} \sqrt{\frac{A}{2}} \frac{1}{(F - F_c)^{1/2}}$ for the FK potential. The reciprocal of this time interval yields an approximation for the wavefront velocity,

$$v(A; F) \approx \frac{1}{2} \sqrt{\frac{A}{2}} \frac{1}{(F - F_c)^{1/2}}; \quad (7)$$

or $v \approx (A^2 - 4)^{1/4} (F - F_c)^{-1/2} = \frac{1}{2} \sqrt{\frac{A}{2}}$ for a FK potential. In Fig. 3 we compare this approximation with the numerically computed velocity for $A = 100$ and $A = 10$.

When the solution begins to blow up, the outer solution (6) is no longer a good approximation, for $u_0(t)$ departs from the stationary value $u_0(A; F_c)$. We must go back to (3) and obtain an inner approximation to this equation. As F is close to F_c and $u_0(t) = u_0(A; F_c)$ is of order 1, we solve numerically (3) at $F = F_c$ with the matching condition that $u_0(t) = u_0(A; F_c)$ at $t = t_0$. This inner solution describes the jump of u_0 to values close to U_3 . During this jump, the motion of u_0 forces the other points to move. Thus, $u_1(t)$ can be calculated by using the inner solution in (1) for u_0 , with $F = F_c$ and $u_2 = U_1$. A composite expansion [21] constructed with these inner and outer solutions is compared to the numerical solution of (1) in Fig. 4.

Notice that (5) is the normal form associated with a saddle-node bifurcation in a one dimensional phase space. The wavefront depinning transition is a global bifurcation with generic features: each individual point $u_n(t)$ spends a long time, which scales as $(F - F_c)^{-1/2}$, near discrete values $u_n(A; F_c)$, and then jumps to the next discrete value on a time scale of order 1. The traveling wave ceases to exist for $F = F_c$. For these field values, discrete stationary profiles $u_n(A; F)$ are found. The above calculations give a normal form of the type $d^2 v_0/dt^2 = (F - F_c) + v_0^2$ instead of (5) for conservative discrete systems (two time derivatives instead of one in (1)). The solution of this equation blows up in finite time as $(F - F_c)^{-1/4}$, which gives a critical exponent of $1/4$ for the wavefront velocity near the critical field.

The approximations to $F_c(A)$ and the wavefront speed provided by the previous asymptotic theory break down for small A . In particular, for the FK potential and $A < 2$, no double zeroes of $2x + A \sin(x) - (F + U_1 + U_3)$ are found for $F = F_c$. What happens is that we need more than one point to approximate wavefront motion. Depinning is then described by a reduced system of more than one degree of freedom corresponding to active points. There is a saddle-node bifurcation in this reduced system whose normal form is of the same type as (5). The jump of the active points after blow up is found by solving the reduced system with a matching condition [22]. As we approach the continuum limit, more and more points

enter the reduced system of equations and exponential asymptotic methods become a viable alternative to our methods.

In conclusion, we have studied depinning of wavefronts in discrete RD equations. The normal depinning transition can be viewed as a loss of continuity of traveling front profiles as the critical field is approached: below the critical field, the fronts become pinned stationary profiles with discontinuous jumps at discrete values u_n . In the strongly discrete limit, the critical field and these fronts can be approximated by singular perturbation methods which show excellent agreement with numerical solutions. The leading order approximation to the wavefront velocity is then correctly given (scaling and prefactor) near the critical field. Depinning transitions for discrete RD equations apparently belong to two different universality classes. In the normal class, the wavefront velocity has a critical exponent $1/2$. For certain nonlinearities, the stationary fronts are continuous functions of the discrete index at zero field. Then the critical field is zero, the depinning transition between stationary and moving fronts is continuous, with a critical exponent 1. This situation is the same as for continuous RD equations and we have called it anomalous pinning.

AC thanks S. Hastings and J.B.M. Cleod for fruitful discussions.

-
- [1] J.P. Keener, SIAM J. Appl. Math. 47, 556 (1987).
 - [2] J.P. Keener and J. Sneyd, Mathematical Physiology (Springer, New York, 1998). Chapter 9.
 - [3] A.E. Bugrim, A.M. Zhabotinsky and I.R. Epstein, Biophys. J. 73, 2897 (1997); J. Keizer, G.D. Smith, S. Ponce Dawson and J.E. Pearson, Biophys. J. 75, 595 (1998).
 - [4] G.G. Guner, Rev. Mod. Phys. 60, 1129 (1988); A.A. Mikhlin, Phys. Rev. Lett. 68, 670 (1992).
 - [5] H.S.J. van der Zant, T.P. Orlando, S.W.atanabe and S.H. Strogatz, Phys. Rev. Lett. 75, 174 (1995).
 - [6] F.R.N. Nabarro, Theory of Crystal Dislocations (Oxford University Press, Oxford, 1967).
 - [7] P.M. Chaikin and T.C. Lubensky, Principles of condensed matter physics (Cambridge University Press, Cambridge, 1995). Chapter 10.
 - [8] M. Locher, G.A. Johnson and E.R. Hunt, Phys. Rev. Lett. 77, 4698 (1996).
 - [9] L.L. Bonilla, J. Galan, J.A. Cuesta, F.C. Mart nez and J. M. Molera, Phys. Rev. B 50, 8644 (1994); L.L. Bonilla, G.P. latero and D. Sanchez, Phys. Rev. B 62, 2786 (2000); A. Wacker, in Theory and transport properties of semiconductor nanostructures, edited by E. Scholl (Chapman and Hall, New York, 1998). Chapter 10.
 - [10] A. Carpio, L.L. Bonilla, A. Wacker and E. Scholl, Phys. Rev. E 61, 4866 (2000).
 - [11] K.K. Ladko, I.M. Itkov and A.R. Bishop, Phys. Rev. Lett. 84, 4505 (2000).

- [12] I. M. Itkov, K. Kladko and J.E. Pearson, Phys. Rev. Lett. 81, 5453 (1998).
- [13] J.R. King and S.J. Chapman, Eur. J. Appl. Math. (2001), to appear.
- [14] B. Zinner, J. Diff. Eqs. 96, 1 (1992); A.-M. Filip and S. Venakides, Comm. Pure Appl. Math. 52, 693 (1999).
- [15] A. Carpio, S.J. Chapman, S. Hastings, J.B. McLeod, Eur. J. Appl. Math. 11, 399 (2000).
- [16] J. Frenkel and T. Kontorova, Phys. Z. Sow. Un. 13, 1 (1938).
- [17] If we have $l_n(0) = u_n(0)$ such that $u_n = u_{n+1} - 2u_n + u_{n-1} + F \text{Ag}(u_n)$, and $l_n = l_{n+1} - 2l_n + l_{n-1} + F \text{Ag}(l_n)$, then $l_n(t) = u_n(t)$ for all later times. $l_n(t)$ and $u_n(t)$ are called sub and supersolutions, respectively. See Ref. [15].
- [18] R. Hobart, J. Appl. Phys. 36, 1948 (1965).
- [19] V.L. Indenbom, Sov. Phys. { Cryst. 3, 193 (1958).
- [20] J.B. McLeod, private communication.
- [21] L.L. Bonilla, J. Statist. Phys. 46, 659 (1987).
- [22] A. Carpio and L.L. Bonilla, unpublished.

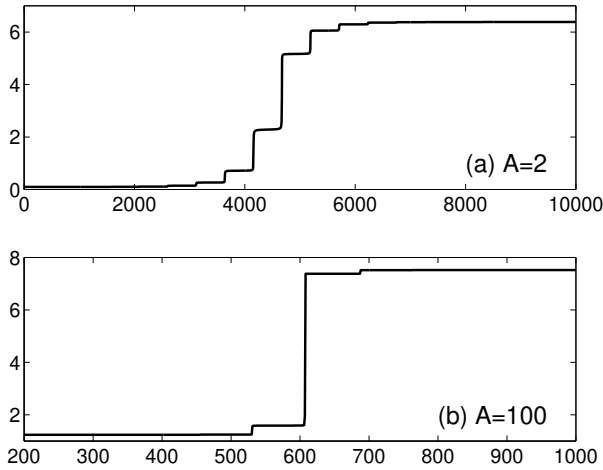


FIG. 1. Traveling wavefront profiles near $F = F_c$ for the FK potential and: (a) $A = 2$, (b) $A = 100$.

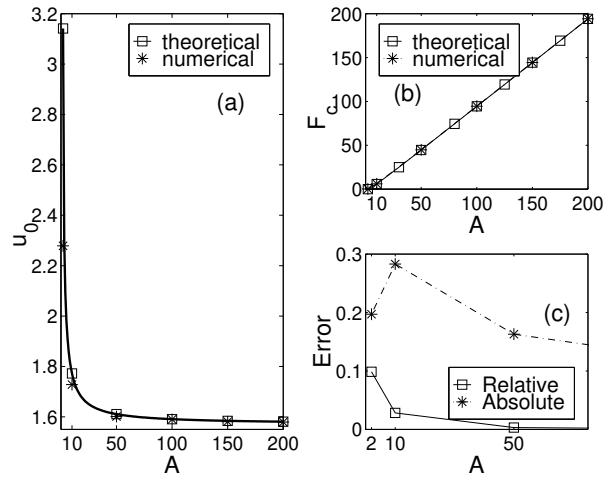


FIG. 2. (a) $u_0(A; F_c)$; (b) Critical field as a function of A ; (c) Absolute and relative errors in $F_c(A)$.

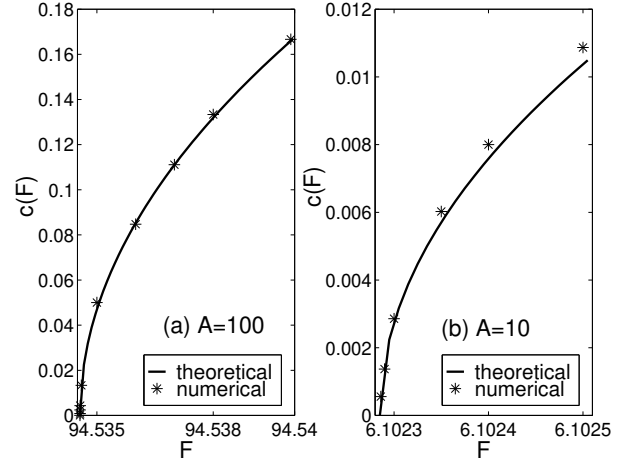


FIG. 3. Wavefront velocity versus F near $F = F_c$ for the FK potential and: (a) $A = 100$, (b) $A = 10$.

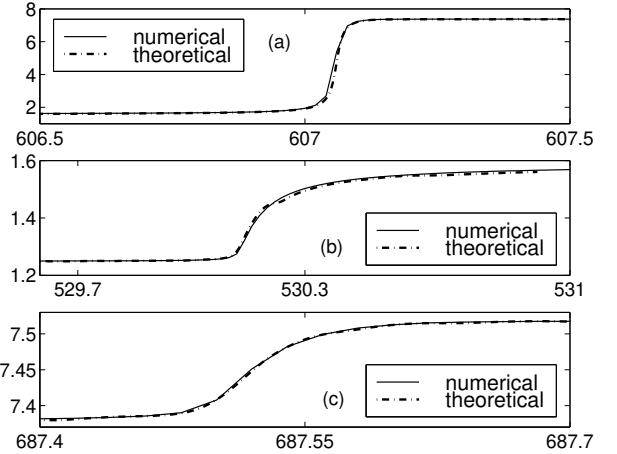


FIG. 4. Wavefront profiles near F_c for the FK potential and $A = 100$. We show the three largest jumps in Fig. 1 (b).